TITLE PROJECT:

pH sensitive nanoparticles, with nanodiamonds as a drug delivery system of diazoxide.

Detection of the ROS via Diamond Magnetometry

Name student: Laurens Bosscher Navarro

S-number: S4936779

Name of company/department

UMCG- Bioimaging & Bioanalysis

Period: 18/04/2022 - 08/07/2022

Internship

Supervisor:

Dr. Romana Schirhal, UMCG Bioimaging & Bioanalysis

Kaiqi Wu UMCG Bioimaging & Bioanalysis

Examiner:

Dr. Romana Schirhal, head of the UMCG Bioimaging & Bioanalysis

Dr.prof. Brandon Peterson, UMCG Faculty of Medical Sciences

Table of Content

Abstract:

The potential for nanodiamonds in the delivery and sustained release of anticancer drugs has been recently demonstrated due to their biocompatibility, stable structure, and highly modifiable surface chemistry. The cellular response, however, to these nanomedicines was rarely studied. Lately, fluorescent nanodiamond (FND) containing Nitrogen-Vacancy (NV) defect centres was successfully utilized to monitor the intracellular free radicals' level by optical ways, which is also called diamond magnetometry.

This study aims to investigate the cellular oxidative stress when cells are treated with nanomedicine using diamond magnetometry. Specifically, hyperbranched polyglycerol (HPG) was modified to the nanodiamond surface by polymerization to increase the stability of FND in physiological environment, and a pH-sensitive structure, carboxy-dimethylmaleic anhydride (DMA), was covalently conjugated to FND surface. FT-IR and DLS were used to characterize this nanocarrier. This pH-sensitive nanodiamond drug carrier exhibits excellent stability in the physiological environment with 135 nm diameters. We found that the modification of diazoxide on nanodiamond can recover the uptake of nanodiamond by triple negative breast cancer cell lines MDA-MB-231, which was mostly blocked by the modification by hyperbranched polyglycerol. In this project, we also examined the cellular toxicity and cellular oxidative stress of Diazoxide against MDA-MB-231.

Though, there are still improvements on this project, the current modification on nanodiamond and basic research on diazoxide provides the feasibility to use diamond drug delivery platform as a drug screen tool based on cellular response and diamond magnetometry.

Introduction:

The production of free radicals or reactive oxygen species (ROS), in cells is a necessary process which involves immunological signalling (secretion of cytokines) and cell pathways. These pathways may include the NADPH oxidase NOX2 activation [1], which will provoke a generation of superoxide radicals in the lumen of endosomes, phagosomes and the extracellular space.

The generation of free radicals is provoked as a necessary process for the respiration of the cells and other cell processes, but it can develop into toxic substances in high quantities as an example the superoxide can rapidly become peroxide and other type of radicals, which will cause damage towards DNA, proteins and lipids, as well as interfering in the electron transport of the cell [1], inducing the death of the cell and the surrounding parts.

As commented the respiration depends on the use of oxygen species, by the mitochondrial electron transport chains, as a consequence of the electron escape during adenosine triphosphate synthesis (ATP) [2].

Having the presence of the free radicals in the body is part of the homeostasis state in which it must maintain a balance between these species and the antioxidants, if the balance is broken it can develop into oxidative stress towards the body, and be able to generate: inflammatory diseases, ischemic diseases, neurological disorders such as Alzheimer's disease or Parkinson's disease [3].

Observing Figure 1 there are two sources from where ROS species can originate from, either way, if the previous balance mentioned is broken the generation of oxidative stress will occur, following the subsequent path observed in Figure 1 [4].

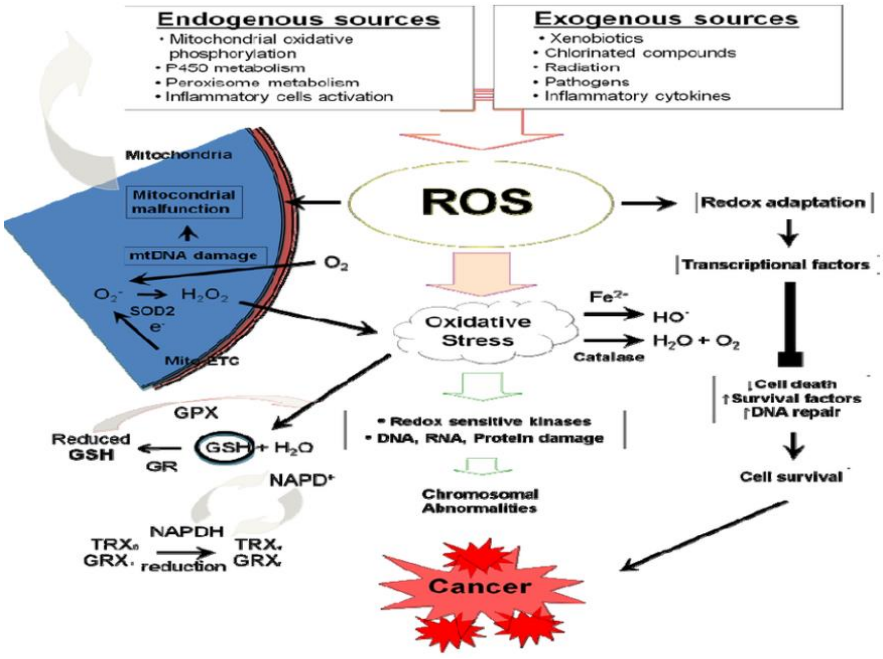

Figure 1: Signalling pathways induced in the ROS production and oxidative stress [4]

Herein there is a relevant interest on observation and analysis, of the development and creation of the free radical species and ROS. The available techniques now a days have two methods of being able to measure these species, by indirect and direct measurements.

On one hand the indirect it bases itself on the detection over the damage done to the lipids and DNA by the free radicals, thus the analysis is based on quantifying the damage observed and giving a quantitative estimate of the free radicals [1]. But this lacks spatial resolution and specific analysis of the radicals itself.

On the other hand, there are the direct methods, that are composed of fluorescence or spin label proves, which a form visible compound after reacting with the free radicals, giving spatial resolution of where the ROS is detected. But these methods lack from specificity, because normally tend to react with the ROS species, and there can't be real time resolution from them, provoking to do the analysis at different time points of analysis without the possibility of continuous study. Such methods are DCFDA, MitoSOX, or MitoTracker red CM-H2Xros [2].

It is certain that there are some dyes which are specific to free radicals, as the hydroxyterephtalic acid (HTA) or the DAF-2, but those suffer from a great disadvantage, which leaves the sample with photobleaching and react reversibly with ROS, showcasing the development of the sample over time, rather than the current state [2].

Observing the current techniques there is a lack for one that can provide with spatial resolution, free radical quantification, and specificity over time, without interfering with the sample and the continuity of the measurement.

One of the focuses of the project is to provide and test a method that can overcome these deficiencies, with the use of fluorescent nanodiamonds (FNDs) and Diamond Magnetometry, based on their biocompatibility and photostability. On the biocompatibility side the FND are able to enter the cell via the Cathryn mediated endocytosis [5], with this system it has been observed that FND can enter either cancerogenic cells and non-cancerogenic cells, FND can escape from endosomes, as they sharp geometry enables them to penetrate the membrane and free themselves from the endosomes[6].

Those advantages provide the FND a platform in which it can be a polyvalent tool in cell analysis systems, adding to it the FND have a paramagnetic feature that can translate magnetic signals into optical ones, because of a modulation in the nitrogen vacancies (NV) inside the nanodiamonds [7]. The NV centres have the ability to detect the surrounding environment and coupled with the fluorescent feature of the FND can change the relaxation time (or T1) of the FND, thus providing a signal that can be analysed.

Therefor with the use of this new technique there is the possibility of measuring the free radicals present in from oxidative stress of the cells. In nanoscale measurements and without the need of destroying the sample in the process. The T1 process called relaxometry, is sensitive to the spin noise, in the case of study over the unpaired electrons in the free radicals [2].

Complementary to the use of this technique, the nanodiamonds will be coupled with a pH sensitive polymer for targeted drug delivery of Diazoxide, which is also the main objective of this project. The polymer will consist of hyperbranched polyglycerol (HPG), as it show high biocompatibility and a layer can be constructed upon de ND via ring opening multi branching [8].

The HPG also serves as a platform for attachment of other substances in the OH radicals that it presents, in this case, there will be an attachment of the 2,3-dimethylmaleic anhydride (DMA), which is sensible to the pH and will change conformations between 7,4 and 6,5 pH [9]. At around this pH the structure of the DMA remains stable but whenever the pH drops from the 6,5 there is a structural change that will cleave the union between the amide group and the drug attached to the DMA, as seen in Figure 2.

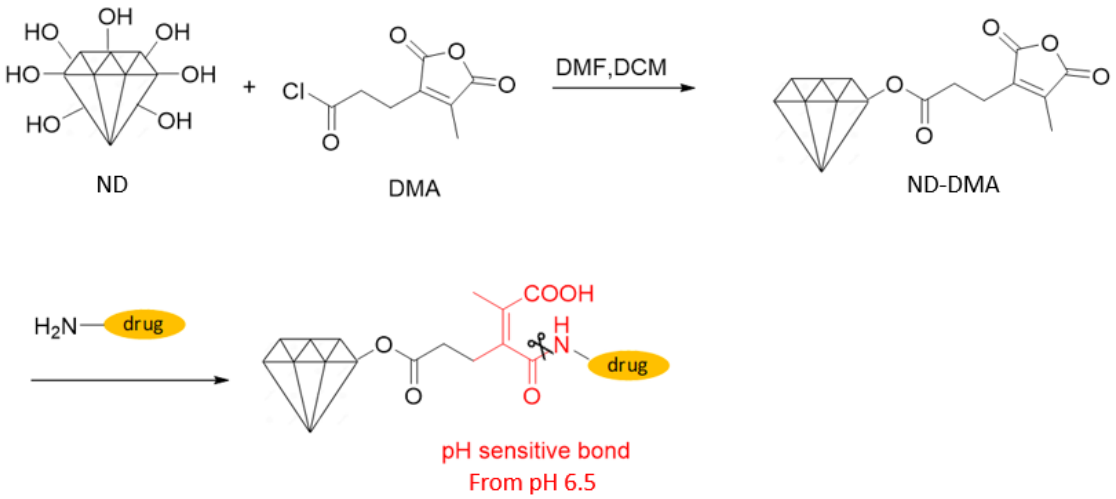

Figure 2: basic sketch over the Nano Diamond modification with the DMA pH sensitive bond and the drug, showing the cleaving of the amide bond below pH 6,5

Having this delivery method for our nanoparticles of FND, is useful in the sense that it can achieve active drug targeting for tumour or cancerous sites, using the EPR effect[9,10] and the acidic environment of tumours around (6,9 to 6,2 pH)[9,11,12], to localize and specifically release the drug on this sites. This differentiation in the pH may change depending on the tumour type, in the case of lung cancer xenografts is 6,5 pH [9], where the drug delivery method would be effective

Diazoxide will be the drug attached to these nanoparticles, as it has the amino group which can link with the DMA polymer, and in the case of fluorescence analysis it won't provide a signal, affecting the analysis in the Diamond Magnetometry.

This drug is a potassium channel opener for the cells, which can affect the proton balance in the cell, creating a disbalance towards the electron transport chain (ECT), affecting the CII complex [13].

The latter effect it's been observed to also has demonstrated neuroprotective effects in cerebral ischemia-reperfusion injury, being able to diminish the levels of reactive oxygen species, decreasing DNA oxidative damage, also showcasing neuroprotective effects [14]. The levels of toxicity of the Diazoxide can be controlled having an IC50 on the CII of 32 µM in rat heart mitochondria[13], modulating this we can generate various levels of stress in the cells, thus serve as a test to the generation of ROS, to observe if the pH sensitive polymer works with this specific drug.

As in previous investigations of the group the feasibility of the pH sensitive link has been tested, but not with the Diazoxide, rather with a fluorescent dye (Alexa Fluor 488 cadaverine), that enabled to test the usage of this pH sensitive polymer activation and feasibility. Which it has been shown to function.

Having observed these properties of the NP, coupled with the advantages of FND imaging and analysis, this project expects to build up a platform from where to lead the further scientific investigation, into further understanding of the oxidative stress and to provide a polymer which can be targeted to the sites of action.

Material & Method:

Cells: MAD-MB-231

- Growth conditions:
  - Culture medium:
    - 93% → DMEM + GLUMAX
      - + 4,5 g/L D-Glucose
      - + Pyruvate
    - 6% → FBS
    - 1% → PLS
  - Temperature: 37 ºC

This MAD-MB-231 are epithelial, human triple negative cancer breast cells[15], this cell line has the characteristic that lacks oestrogen receptor, progesterone receptor and human epidermal growth factor receptor 2 (HER2) expression. As a result of this is classified as claudin-low molecular subtype, this is because it shows a down-regulation of claudin-3 and claudinin-4, and low expression of the proliferation marker Ki-67. As well as, expression of CD44-CD24-/low phenotype[16].

The cell type is chosen because of its cancerous nature as well as its growing properties, having a confluency of 80%-90% over a T-25 plate over the span of 3 days, also they epithelial properties make them suitable for a T plate growth.

Adding to this, it enables the study of nanoparticles and drugs over a cell type which now a days has little treatment options, thus making it possible to understand more about the effectiveness of the approach chosen to the solution.

Nano diamonds

- <u>Diamond cleaning</u>

The nanodiamonds used for the polymer reaction need to have a surface cleaning to leave the surface of the Diamonds with only the desired radicals, COOH and OH. As seen in Figure 3, where the methyl (CH_2 and CH_3) groups are eliminated from the surface, leaving the OH group.

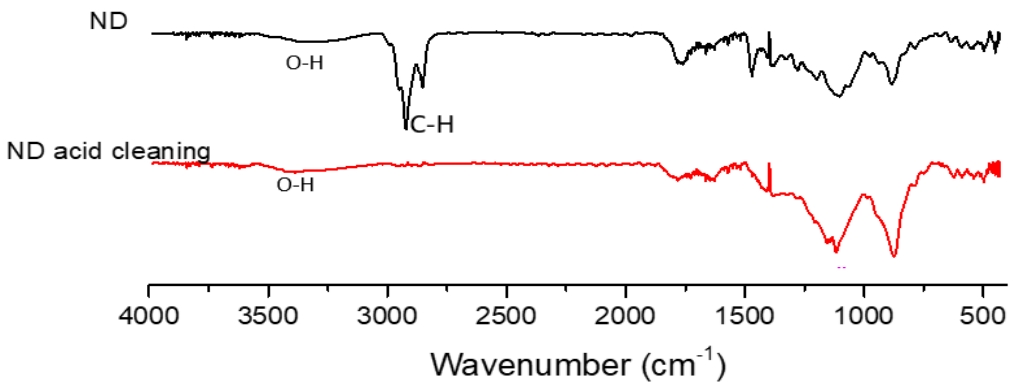

Figure 3:FT- IR spectra comparing the ND and the ND after the acid cleaning

Experimental procedure:

- Nanodiamonds (50-150 nm, 100 mg/mL, 5 mL) were cleaned in a boiling mixture of sulfuric acid (H_2SO_4) and nitric acid (HNO_3) mixed in the ratio of 1:3 (5 mL/ 15 mL) at 140 °C for 3 days to remove unsaturated bond and to get -OH, and COOH group as much as possible.

- After the boiling, mixture was allowed to cool to the room temperature. The acid mixture was diluted in MilliQ H_2O (200 mL), and centrifuge at 20000 rcf, for 20 min. And washed by MQ water twice. Then the pellet was resuspended in MQ water, followed by sonication to get a uniform solution. The acid cleaned NDs were purified by dialysis (MWCO: 3000 Da) against water to remove the remaining acid. Then ND solution was frozen dry to get the powder.

- ND-HPG

Hyper branched polyglycerol (HPG) is a nontoxic polymer, biocompatible, has high solubility in physiological condition and has terminations of hydroxyl groups that are hydrophilic [8,17].This enables this polymer to be a platform where to attach the DMA via hydrogen bond.

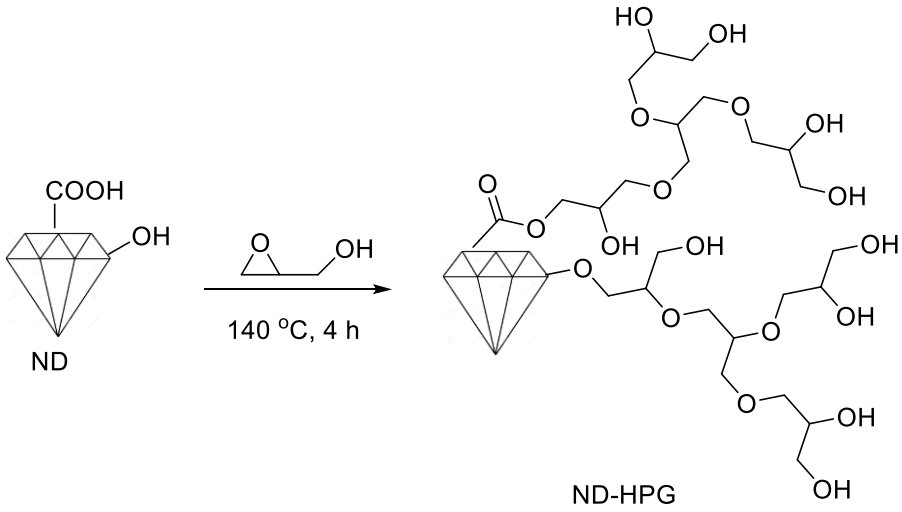

Figure 4: ND -HPG reaction of coupling

Experimental procedure:

- 1,01 g ND was dispersed in 30 mL of glycidol, sonicated to get a uniform mixture for 2,30min.
    - The yield mixture stirred at 140 °C for 4 h under an argon atmosphere, and with a refrigerating coil.

  - Gas exchange done via the usage of a balloon to change the atmosphere towards the argon.
- After reaction, 20 times of Methanol was added to quench the reaction. And the resulted nanoparticles were purified by centrifuge-washing cycle and dialysis against water.
- Argon its used as this gas is not a reactive species thus it won't interfere with the reaction at hand.

- <u>2,3-dimethylmaleic anhydride - (DMA) - pH sensitive – ND-HPG-DMA</u>

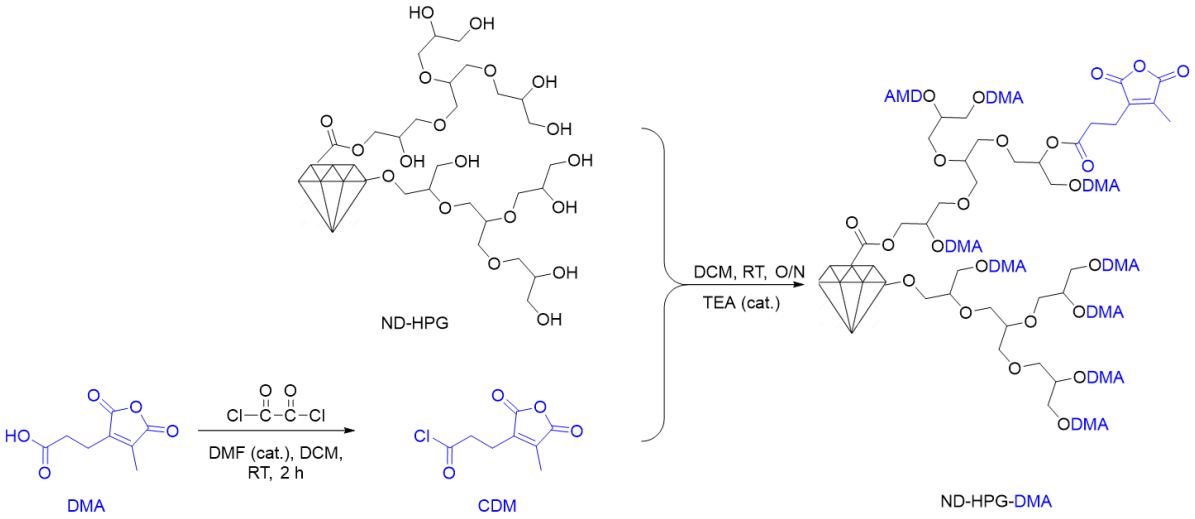

Figure 5: Synthesis of ND-HPG-DMA

The 2,3-dimethylmaleic anhydride - (DMA), is a pH sensitive because of the β-carboxylic amide, as it has a pH responsive hydrolysis[12,18], which allows to cleave the bond with the drug to released when the pH drops from 6.5-6.8 [18,19], correlated with the tumour pH, because of the increased glucose uptake and quick metabolism of the tumour site.

The β-carboxylic amide, of the DMA is stable and negatively charged over the neutral pH (7), having stability on physiological conditions of the body as the pH is around 7,4[11,18,20], but when in contact with the lower pH of the tumour environment its conformation changes and exposes its amino group having a positive charge.

As commented before this mechanism allows the polymer to be an active drug for tumour targeting as the release mechanism will activate when in presence of this acidic pH, thus having a controlled released of the drug gaining on specificity and efficacy, as the drug released is done in site, needing less dosage and a more controlled side effect, because the effect will be targeted.

<u>Experimental procedure</u>:

Under nitrogen atmosphere, DCM (0.276 g, 1.5 mmol) was dissolved in 10 mL dry dichloromethane, and then oxalyl chloride (0.378 g, (0.26 mL) 3 mmol) and a catalytic amount of DMF (40 µL) were added. The solution was stirred for 30 minutes at 0 °C, and then transferred to room temperature for further reaction for 1 h. After the vacuum drying, the

chlorine-substituted DCM was then reacted with ND-HPG (0.5g) in 5 mL of dry dichloromethane with 30 µL of pyridine as the catalyst

- Diazoxide, ND-HPG-DMA-Diazoxide

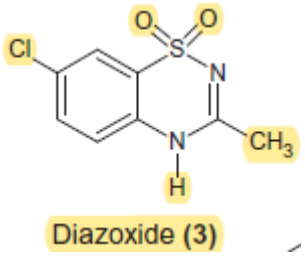

Figure 7: Diazoxide molecule [15].

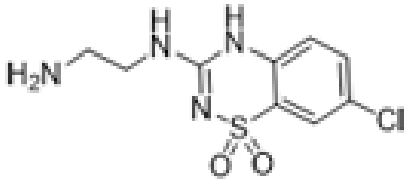

Figure 6: Modified Diazoxide molecule to allow the amide linkage.

The (7-chloro-3-methyl-2H-1,2,4-benzothiadiazine 1,1-dioxide) or so called Diazoxide, is normally used as drug that opens the k^+ ATP channels, is used as a vasodilator vascular smooth muscle cells and as an inhibitor for insulin secretion by the opening of the K ATP channels in the beta cells of the pancreas[21].

It has a chemical structure that allows it to couple with the DMA via the use of an amide bond, this one will open its ring and join with the modified Diazoxide via an amide bond. Leaving out the COOH group, which will be sensitive to the pH, in case the pH drops from 6,5, the amide bond will be cleaved and the Diazoxide released, as shown in Figure 2. In Figure 8 is the reaction followed to link the polymer and the Diazoxide, and Figure 9 showcases where the cleavage is done.

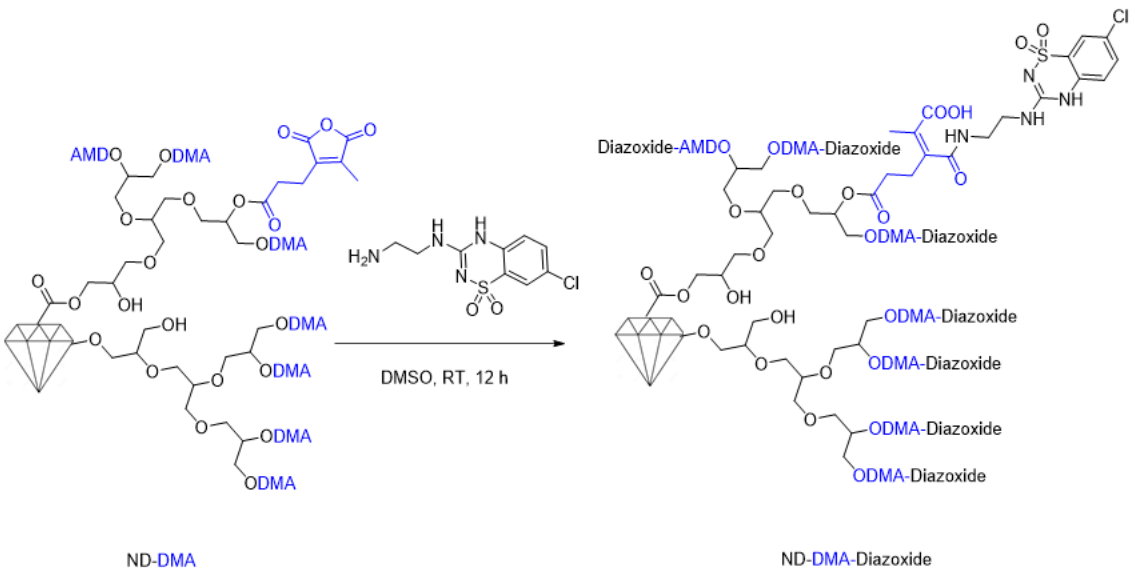

Figure 8: ND-HPG-DMA and modified Diazoxide linkage reaction under DMSO medium

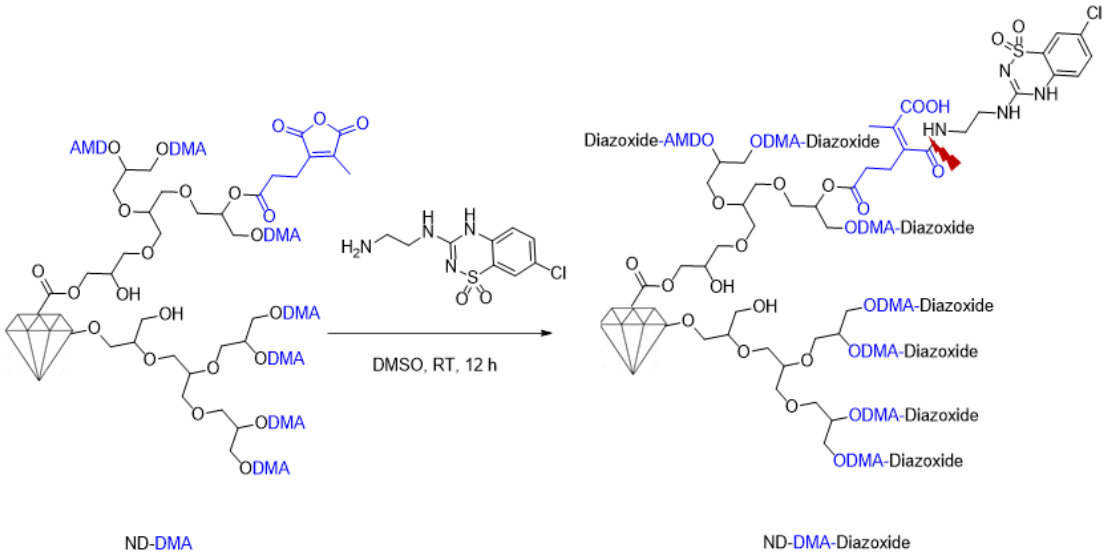

Figure 9: Cleavage on the amide of the DMA and the Diazoxide

Experimental procedure:

- 10,5 mg of ND-HPG-DMA in 1 ml of DMSO, left in 10 min sonication at 60% amplitude and intervals of 5 seconds, the temperature is reduced in an ice bath in order to maintain the bond stable.
- After this, the solution is mixed with 1ml DMSO with 10,1mg of modified Diazoxide.
- Leaved overnight with stirring at room temperature (25°C)
- Vacuum dry, with liquid nitrogen freezing, to obtain the polymer in powder state.

MTT

The MTT analysis is used to observe the viability of cells to the exposure to the polymer or the drugs, via the conversion of a substrate in this case the MTT by the live cells, into the product formazan, which present a purple colour and is insoluble in normal medium, this conversion is mediated by the mitochondrial reductase. After the production of the formazan by the live cells, the medium is changed to DMSO to solubilize the composite and evaluate its production via spectrophotometer having two peaks in 490nm and 570nm[22].

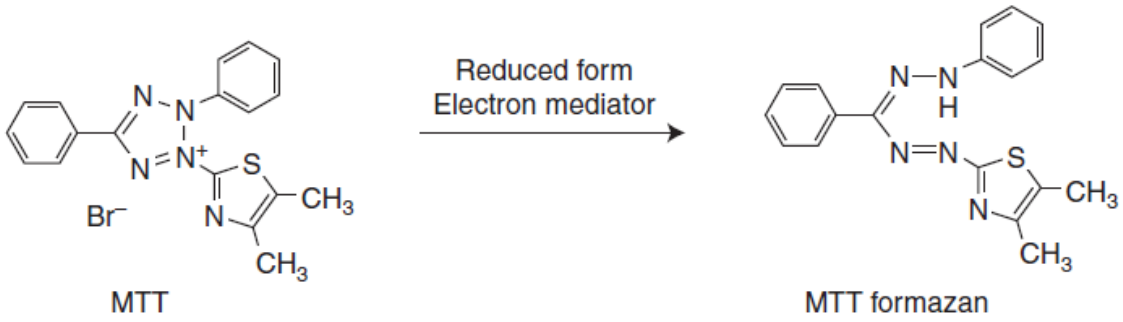

Figure 10: reduction of the MTT into MTT formazan [22]

Experimental procedure:

- Using a 96 plate well with a cell density of $8x10^3$ cell/ml, seed the wells needed in a quantity of 150 µl in DMEM GLUMAX medium, let cells grow overnight
- Depending on the experiment if polymer or drug, extract previous medium, rinse with PBS, and add the desired quantities to be evaluated with in DMEM medium.
    - In the case of Diazoxide drug the evaluation of the viability must be done after 48-72h.
- After the incubation is done, 20 µl of MTT is added to each well and is left for 3h incubation time (37 ºC). Avoiding the irradiance light, as MTT is a light sensitive reactant.
- Extract previous medium and add 150 µl of DMSO to dissolve the Formazan formed.
- Evaluate results in spectrophotometer at 490nm or 570nm

Experiments:

1- Free Diazoxide concentration:
    a. 10.000 µM
    b. 7500 µM
    c. 5000 µM
    d. 2500 µM
    e. 1000 µM
    f. 500 µM
    g. 100 µM
2- FND-HPG-DMA-Diazoxide with dilution of 5 times from the maximum concentration tested
    a. 5 mg/ml
    b. 1 mg/ml
    c. 0,2 mg/ml
    d. 0,04 mg/ml
    e. 0,008 mg/ml

DCFHDA general ROS

The DCFHDA is a general oxidative stress (ROS) indicator in cells, this reactant diffuses into cells and reacts with the oxidative species giving a fluorescent reading, inside the cells the acetate groups are cleaved by the cell estearases (before the acetate groups are taken out the reactant is not fluorescent) and the thiol chloromethyl reacts with the glutathione and other types of thiols.

This oxidation process is what gives out a green fluorescent calcein species, which stays in the cell and can be read via a fluorimeter. Having a fluorescence excitation and emission on 492–495/517–527 nm[23].

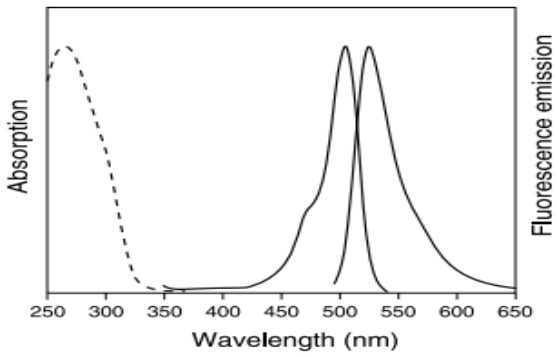

Figure 11: Absorption spectrum of reduced dye (discontinued line (---)) and absorption/emission spectra of oxidized dye (solid

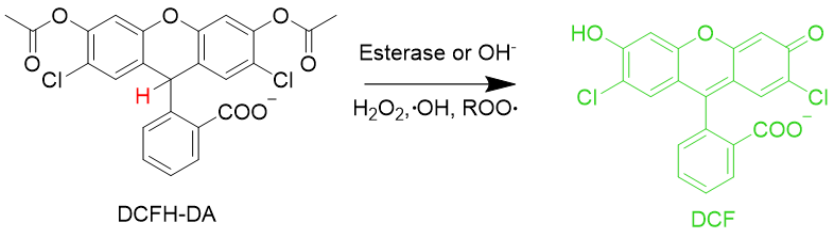

Figure 12: DCFH-DA structure and reaction with the ROS system transforming into DCF

In this experiment one of the samples is going to test out eh Nano Diamonds in conjunction with the Diphenyleneiodonium(DPI), which is a ROS inhibitor via de NADPH oxidase, quinone oxidoreductase, cytochrome P450 and nitric oxide synthase[24].

The usage of this inhibitor serves as a control that the ND don't give out signal in the DCFDA, as the ROS system will be inhibited, thus in theory a low signal should be observed.

As a positive control H2O2 is used, as it will induce ROS system, therefore evaluate the two different parts of the spectrum, the negative and positive control.

Experimental procedure:

Tested in a 96 well plate:

In DMEM GLUTMAX medium

- 1 control group
- 1 positive control with H2O2 (0,01%)
- 3 different concentrations of Diazoxide
    - 500 µM
    - 750 µM
    - 1000 µM
- 3 Diazoxide+ DPI (2 µM)
    - 500 µM
    - 750 µM
    - 1000 µM
- 1 with NanoDiamonds (7,5 µg/µl)

- DCFHDA concentration 10µg/ml
- Cell density per well 8x10³ cell/ml

The cells are grown in a 96 well plate, left overnight to grow, the next day 150 µl of the different solution are placed on each corresponding well, and incubated for 48h (let the Diazoxide react). After this, remove previous medium, wash with PBS, and add the DCFHDA, let react for 1 h. Then, remove the positive control medium and add the 0,01% H2O2, let react for 1h.

Clean all the wells and replace with DMEM, then analyse the samples on a fluorimeter.

CLSM-Confocal Lateral Scanning microscopy

Observation of the fluorescence of the DCFHDA and, and the analysis if the HPG and diazoxide FND can change the uptake efficiency of FND by MDA-MB-231 cell line

CLSM, allows to observe cells in great detail as well as the localization of labelled molecules in cells.

In this case it will be used to assess the functionality of the DCFDA as well as the uptake of the Fluorescent Nano Diamonds (FND) inside the cells and observe if it changes depending on the HPG and the diazoxide.

Experimental procedure:

Uptake efficiency of FND, FND-HPG, FND-HPG-DMA-Diazoxide:

- 1 mL cell culture medium containing FND, FND-HPG, or FND-HPG-DMA-Diazoxide (1 µg FND equiv.) was added to cells (8x 10^4/dish) in 35 mm petri dishes (Glass bottom, Greiner Bio-One).
- After 4 hours incubation, the cells were washed twice with PBS and fixed using 4% paraformaldehyde solution for 15 min, followed endosomes using EEA1 monoclonal antibody (4 µg/mL, Thermo Fisher), goat anti-Rabbit IgG (H + L) cross-adsorbed secondary antibody, and Alexa Fluor 405 (5 µg/mL, ThermoFisher), respectively.

EEA1 monoclonal antibody for the endosomes[25]

- EEA1 is a gene which appears in early endosomes, thus being the target for the primary antibody to attach to.

Goat anti-Rabbit IgG (H+L) secondary antibody attached to the EEA1[26]

- Will attach to the primary antibody, giving out fluoresce

Alexa Fluor 405, is the conjugate of the Goat anti-Rabbit IgG (H+L), which will give the blue fluorescent colour.[26,27]

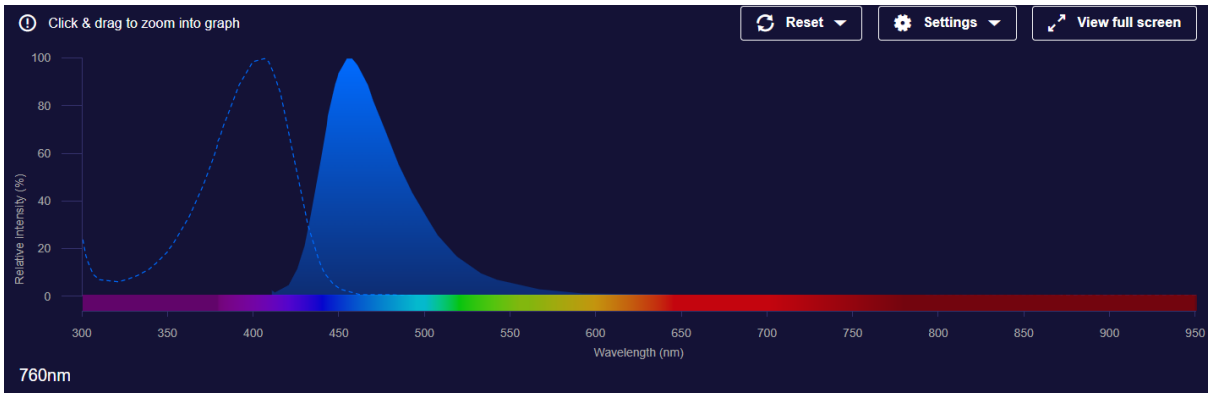

Figure 13: Alexa Fluor 405 Fluorescence spectra[27]

The cells were then imaged using a confocal laser scanning microscopy (Zeiss 780). FNDs were detected at Ex/Em = 561/659 nm, stained endosomes at Ex/Em = 358/461 nm. The cellular morphology was recorded by differential interference contrast (DIC). Images were analysed using FIJI to determine the relative position for diamonds and endosomes.

DCFDA:

In order to check if the DCFDA works, two experiments were devised to observe its functionality, on a first step with two 35 mm petri dishes (Glass bottom, Greiner Bio-One) with a cell density of 8 x 10^4 cell/dish, a negative control for DCFDA and a H2O2 0,01%, positive control.

As well as an evaluation of the interference of the DMEM medium, as it presents a red tonality which may affect the reading of the fluorescence, changing the medium when analysing the samples to 2% FBS and PBS. Using a cell density of 1 x 10^5cell/dish.

DLS

Size of the particles ζ-potential, observe stability of the ND in water and PBS

With the use of DLS the size and the ζ-potential of the ND with different polymer modifications can be measured, in this case it will serve to observe the homogeneity of the sample with the PDI, as well as the aggregation in different mediums and types of nanoparticles.

DLS to be able to analyse the size of the particles uses the principle of the Brownian motion, which defines as the random motion of a particle due to its constant collision with the solvent particles. Because the movement of the particles depends on its own size, smaller particles have higher mobility than larger ones, which can be detected with the diffusion coefficient[28].

The diffusion coefficient can be obtained via the scattering of a laser beam, which will impact with the different nanoparticles, resulting in fluctuations on the intensity. With the use of autocorrelation, the fluctuation of the intensity is observed, depending on the fluctuations and the correlations between themselves the PDI value is obtained and will give a value between 0 and 1, 0 being no similarity and 1 perfect similarity.

On the other hand, in the case of the ζ-potential, identifies the charge of the nanoparticle in the boundary layer between the ND and the solvent, this charge is affected by the conductivity and the pH of the solvent, but also evaluates the stability of the ND in the solvent itself.

The DLS can't measure the ζ-potential directly, it must determine the electrophoretic mobility and then with the use of the Smoluchoswski relation obtain the ζ-potential. With the use of Phase Analysis Light Scattering (PALS), the phase shift is measured, and as the phase shift is linearly dependent on the time and frequency shift, it enables to operate the frequency shift to obtain the particle velocity. With the Fast Field Reversal (FFR) technique the DLS can obtain the electrophoretic mobility[29].

Experimental procedure:

Tested ND and ND-HPG in miliQ water and in PBS, to observe its size, ζ-potential, and stability.

At the same time ND-HPG-DMA-Diazoxide is going to be evaluated, to compare the results to ND and ND-HPG

1- ND→ 5µg/ml on 1 ml of miliQ water and 1 ml PBS
2- ND-HPG→ 5µg/ml on 1 ml of miliQ water and 1 ml PBS
3- ND-HPG-DMA-Diazoxide→ 5µg/ml on 1 ml of miliQ water

FT-IR

Fourier transform infrared serve to observe the composition of certain molecules, this is done via the principle that the molecules absorb the irradiated light, the different structures present in the molecule will change the quantity and the wavelength absorption of the light. This absorption is done via the excitation of the structure and the vibrations of the different molecules will give out a unique read out, in the spectra of the light irradiated.

The most important factors in infrared are the dipole moment, the mass of the atoms and the type of molecular absorption. And only certain types of movement between the structure of the molecule are going to be visible in the FT-IR analysis, such as scissoring, asymmetrical stretching, asymmetrical wagging, or twisting.

This technique is specially used as it doesn't destroy and its relatively fast in comparison to other ones available, presenting a high sensitivity and precision.

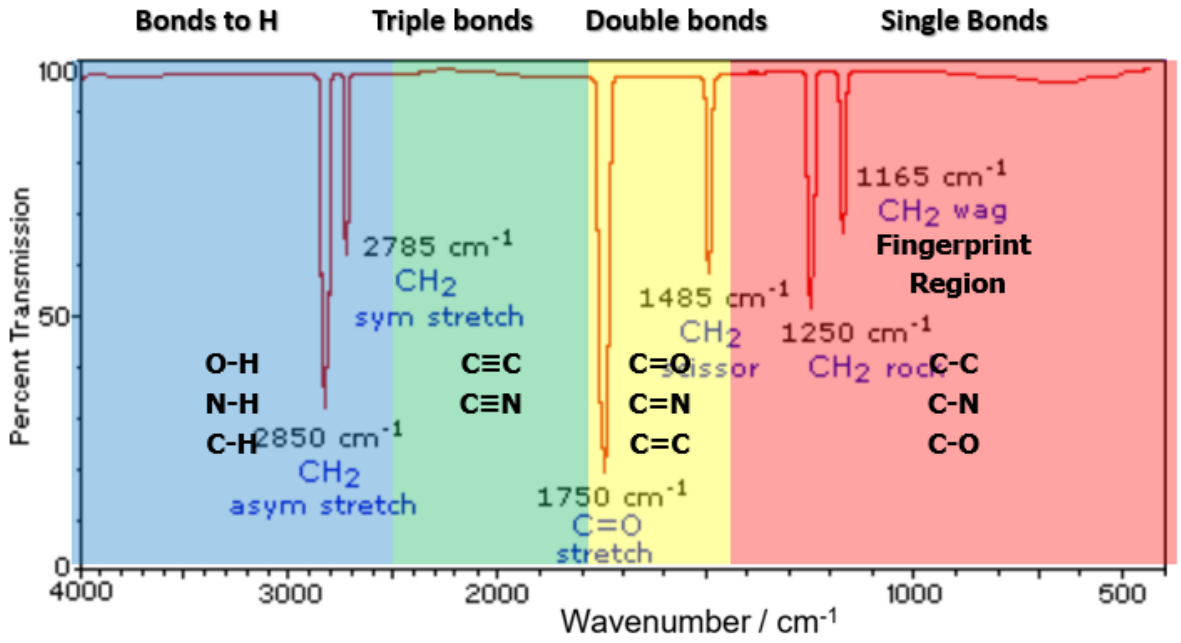

Figure 14: FT-IR spectra and output depending on the type of bond

Experimental procedure:

Analysis of ND-HPG, ND-HPG-DMA and ND-HPG-DMA-Diazoxide

- With the use of a pellet maker, 2 µg of each sample is taken and mixed with 100 mg of KBr (won't give signal under the FT-IR)
- Both are mixed in a mortar until a fine powder is obtained
- Afterwards the powder is compressed to obtain a pellet that can be analysed, this pellet must present a high degree of transparency (to let light get through the sample)

Diamond magnetometry

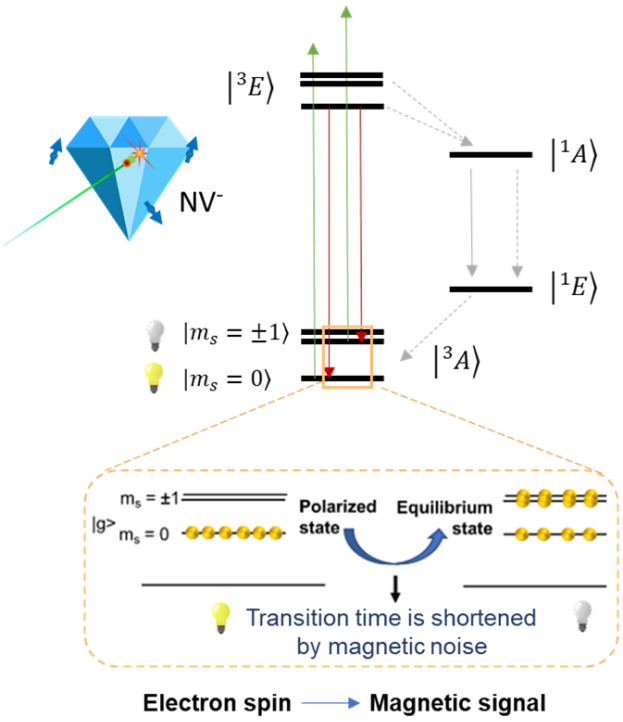

Figure 15: Principle of diamond magnetometry

Basic photo physics of relaxometry that is relevant for this work is explained using Figure 15. NV defects embedded in FNDs can be pumped into the optically brightest polarized state under a continuous laser illumination where most of the electrons are populated in the $|g\ m_s = 0$ energy state. Once the laser is turned off, the optically brightest polarized state of the NV center is lost and electrons transition back to their original equilibrium states $|g\ m_s = 0$ and $m_s = \pm 1$. The time required for the transition from the polarized state to the initial unpolarized equilibrium state is dependent on the magnetic noise around the NV defect. As unpaired free electrons of intracellular free radicals offer magnetic noise, they alter this transition time. In particular, the higher the free radical concentration around the NV center, the higher is the magnetic noise hence shorter is the transition time and vice versa. As a result, the transition time is a direct measure for the amount of cellular free radicals in the vicinity of the NV center. We quantify the transition time between polarized and equilibrium state via measuring spin-lattice or T_1 relaxation.

Results and Discussion:

FT-IR

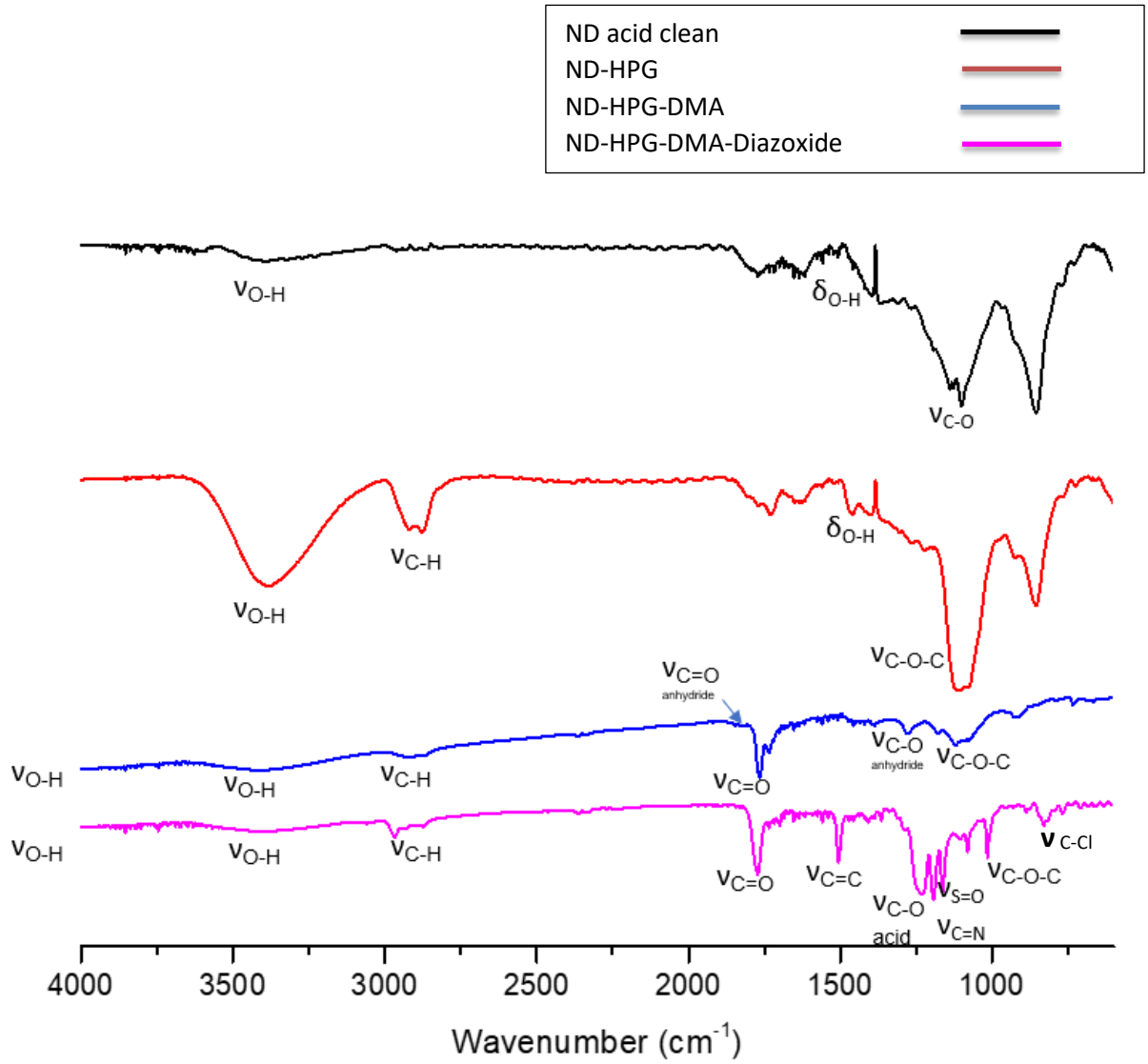

*Figure 16: FT-IR spectra results, of the ND acid clean, ND-HPG, ND-HPG-DMA and ND-HPG-DMA-Diazoxide. With vibrational modes **ν** (stretch) and δ (scissoring).*

From the results obtained from the FT-IR we can characterize the molecules synthetised and observe if the different synthesis of the polymer and its modifications have been successful.

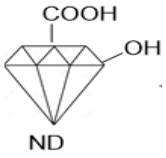

Figure 17: ND structure

On the first case, the ND with acid cleaning, it has been successful as the presence of other molecules rather than the COOH and **δ & ν** OH, such as methylated structures as seen in Figure 3, are not present.

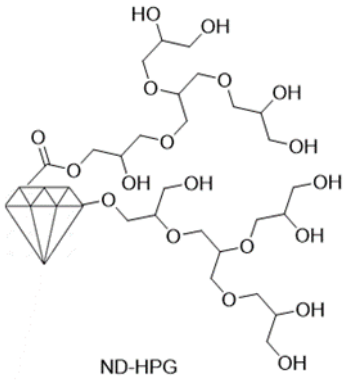

Figure 18: ND-HPG structure

Observing the ND-HPG, the FT-IR shows the addition of the HPG via the higher quantity of OH and C-H bonds present in the different signals detected, meanwhile the structure of the ND remains. With the addition of the **ν** C-O-C bond from the HPG structure of the polymer which also appears near the range of the C-O range.

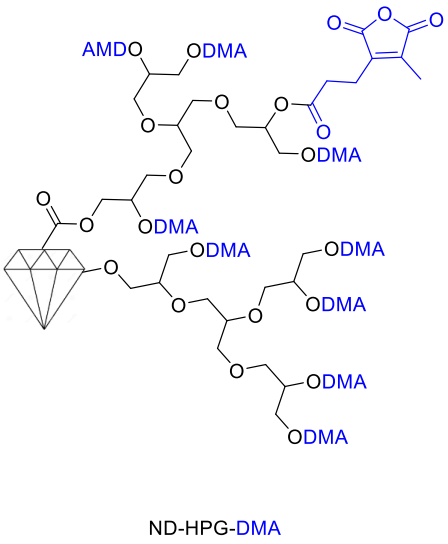

Figure 19: ND-HPG-DMA structure

The DMA attaches to the ND-HPG from the hydroxyls in the radicals of the HPG polymer, thus its presence in the in the signal is reduces as seen in the IR spectre. As the attachment of the DMA has been successful its observable that the bonds from the DMA ring are present, such as **ν** C=O, **ν** C=O anhydride (from the DMA ring), C-Cl and C-O anhydride.

Resulting in the successful addition of the DMA without impurities in the structure, as all the signals recognized where expected in the structure of the ND-HPG-DMA.

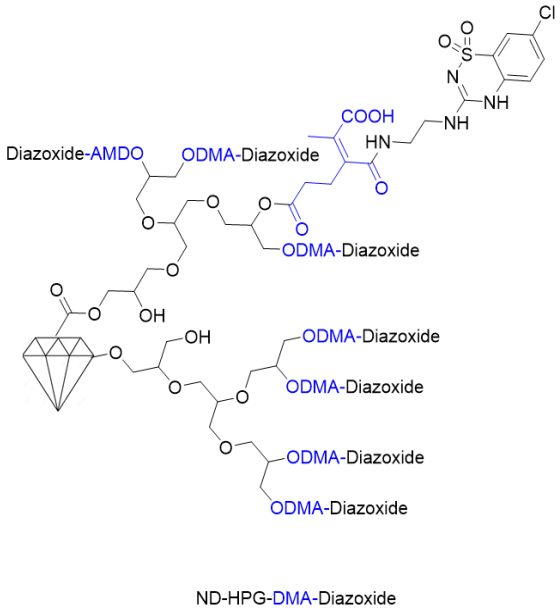

Figure 20: ND-HPG-DMA-Diazoxide structure

Lastly the polymerization of the Diazoxide coupled to the DMA via an amide bond, which also opens the ring structure in the DMA leaving the COOH exposed, which is the pH sensitive factor of the DMA, as below the 6,5 pH it will cleave returning to the ring formation, freeing the Diazoxide.

The signals observed are in accordance with the Diazoxide as now the presence of N and S bonds are altering the IR spectre, as the bonds observed are **ν** C-Cl **ν** C-O acid (ring opening in the DMA), **ν** C=N, **ν** S=O (sulfone group from the Diazoxide) and **ν** C=C (from the ring in the Diazoxide).

In the case of the C-Cl as in inside the Diazoxide ring the signal observed could also be the bending vibrations of the C-H of the benzene ring (880-680 cm^{-1}). Having considered this, all the molecules localized in the signal pertain to the Diazoxide.

Having observed the different result in the FT-IR, the synthesis of the polymer has been successful as the signals corelate to the molecular structures expected.

Even though, the FT-IR of the ND-HPG-DMA and ND-HPG-DMA-Diazoxide, should be repeated as the intensity is not high. Being there improve that factors, thus improving the analysis.

In addition, the gold standard for chemical structure analysing is nuclear magnetic resonance spectroscopy (NMR). However, to analyse the structure on nanoparticles precisely is hardly possible. Thereby, X-ray photoelectron spectroscopy (XPS) and thermogravimetric analysis (TGA) are normally used to confirm the specific chemical groups through their binding energy, and to analyse the amount of modified molecules by calculating their weight losing at different temperatures, respectively. And in our case, XPS and TGA analysis are still under processing.

DLS

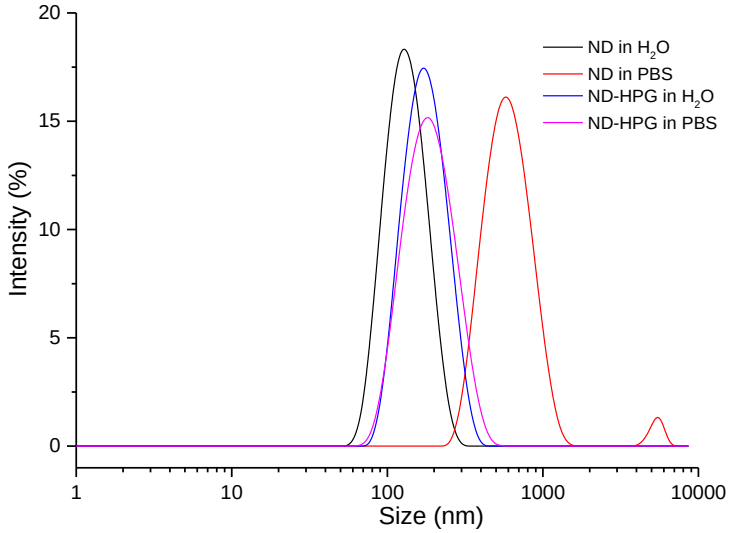

Figure 21: DLS size measurement of ND and ND-HPG in MilliQ water and PBS

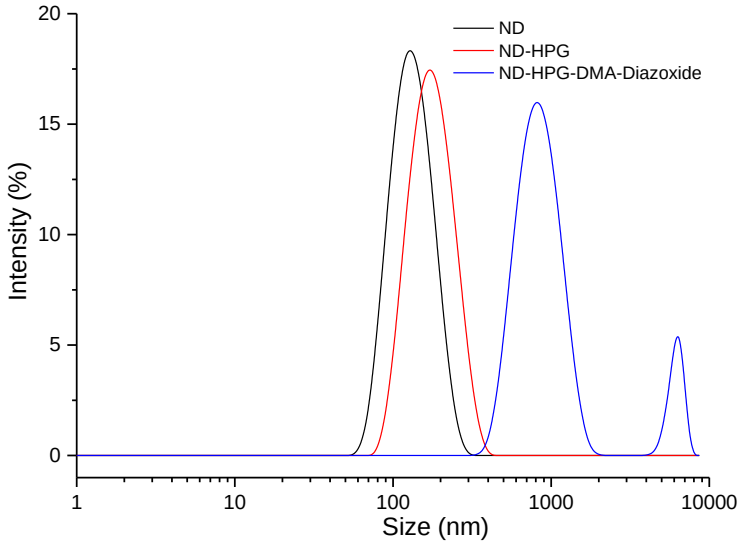

Figure 22: DLS size measurement of the ND, ND-HPG, and ND-HPG-DMA-Diazoxide in MilliQ water

Table 1: DLS results with the standard deviation, over ND, ND-HPG and ND-HPG-DMA-Diazoxide, on Size (nm), PDI and Z-potential (mV)

	Size (nm)	*PDI*	*ζ -potential (mV)*
ND (MQ)	125,2 ± 0,1414	0,090 ± 0,028	-32,3 ± 0,778
ND (PBS)	638 ± 1,556	0,238 ± 0,015	-
ND-HPG (MQ)	166 ± 0	0,077 ±0	-2,76 ± 0,820
ND-HPG (PBS)	173,5 ± 0	0,106 ± 0	-
ND-HPG-DMA-Diazoxide (MQ)	865 ± 65	0,5 ± 0,2	-

The result obtained (Table 1) show that there is a big difference between the ζ -potential of the ND and the ND-HPG, this is due to the surface charge, in the case of the ND the surface is covered by groups OH and COOH, in comparison to the ND-HPG which haves the HPG attached to the nanodiamonds, having a bigger size and in the radicals OH, but these offer a lesser charge to the surface, as the branched out OH is in lesser concentration as in the nanodiamonds, having a ζ-potential value near to 0.

Both NP in water solvent, have a monodisperse structure, as seen in the PDI, meaning the size remains constant with the different NP showing no aggregation.

Surface charge takes relevance when observing the differences in size when both samples are placed in PBs in Figure 21, as observable the ND in PBS increases in size as well as in the PDI, where the ND shows to be more polydisperse, in comparison to the ND-HPG that there is no big change on either size or PDI. This is caused by the differences in surface charge of both NP, as ND is more surface charged the lack of interaction with the PBS, makes it aggregate, observing the size increase and as well as a little peak in the curve over the 1500nm mark.

HPG confers an advantage to the NP, as remains stable in both solvents without aggregation, showing a possible advantage on physiological conditions as well.

Apart from this, observing the increase in size of the ND, and the ND-HPG we can see the polymerization of the nanodiamonds has been effective, even though there is a need to characterize it to observe if indeed what is attached is all HPG.

Shifting to the Figure 22 and the results on Table 1, the ND-HPG-DMA-Diazoxide has a bigger size and PDI of more than 0,5, causing it to have higher aggregation, seen also in the Figure 22 in the peak over the 1500nm. This is caused because the drug is hydrophobic, and thus the high concentration of it on the surface provokes the aggregation of the NP, which is a problem, because generates a polydisperse and big sample, in comparison of a monodisperse one.

This factor can be modified with a reduction of the Diazoxide on the surface of the NP or using PEG-NH2, to increase the hydrophilic properties of the NP, which will help stabilize the NP into a more monodisperse distribution and not aggregate.

CLSM

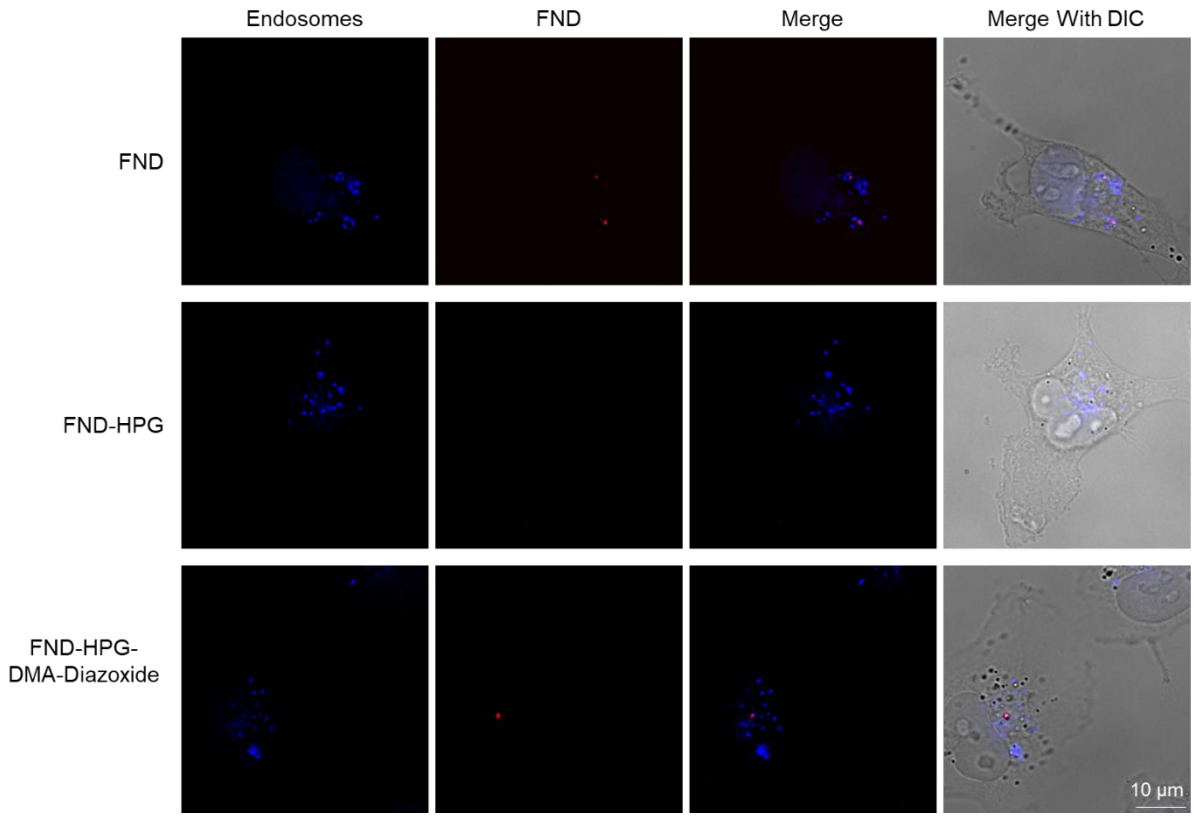

Figure 23: CLSM picture of MDA-MB-231 cells with EEA1 monoclonal antibody, Goat anti-Rabbit IgG (H+L) secondary antibody with Alexa Fluor 350, colour blue=endosomes, red colour FND (fluorescent nano diamonds)

On figure 23, its show the results obtained from the cell marking for endosome detection (blue) as well as the nanoparticle location (red dot). The FND can penetrate into the cell and locate themselves over the endosomes as seen in the first row of images where the merge of the two pictures showcases this.

On the other hand, the FND-HPG it seems to inhibit the cellular uptake as there are no nanoparticles present inside the cell.

FND-HPG-DMA-Diazoxide though doesn't inhibit the uptake into the cells as we observe NP on the endosomes of the cell, but due to aggregation and instability of the NP, the uptake is less than in FND.

The results conclude that the FND and further modifications of the nanoparticles can enter inside the cell and remain in, but further improvement should be made to augment the uptake, such as augmenting the hydrophilicity of the NP, via modification of the polymer.

MTT

The first experiment done the data set presented a high dispersion to be accepted as good, therefor there was a change in the MTT to test if the previous one used was expired. In this case was as the result appear to be more homogeneous than before.

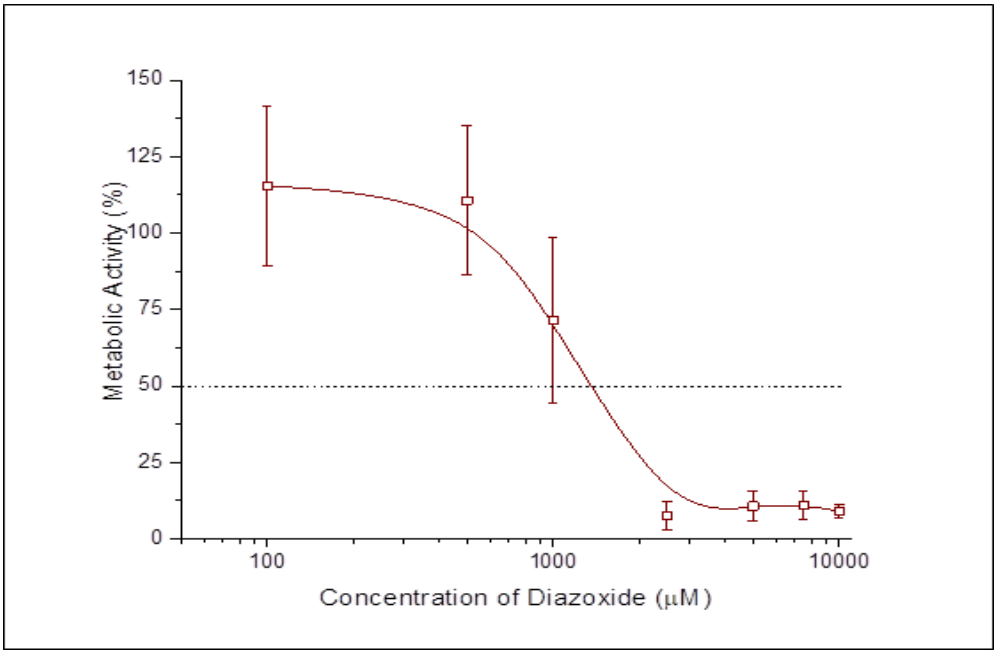

Figure 24: MTT for the different concentration on free diazoxide on MDA-MB-231 cells, error bars standard deviation of the results

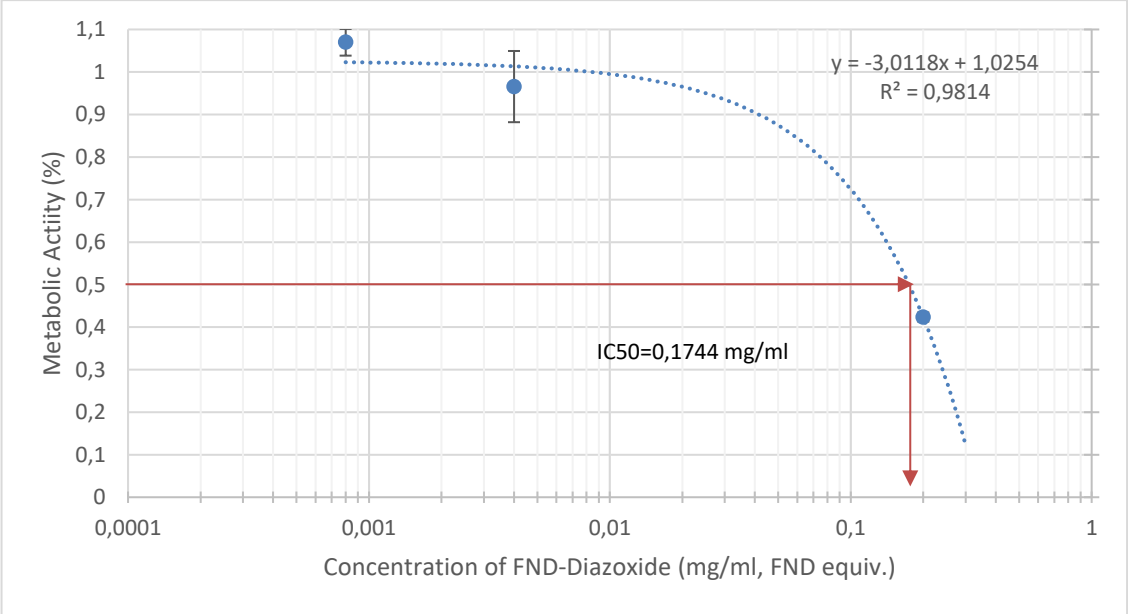

Figure 25 MTT for the different concentration on FND- diazoxide on MDA-MB-231 cells, error bars standard deviation of the results

Figures 24 and 25 show the results obtain on both experiments of the MTT analysis, it was used to observe the different IC50 of the MDA-MB-231 cells to the presence of free diazoxide and the diazoxide attached to the FND. Observing the cell metabolic activity, which correlates

with survival of the two compounds in different concentrations in comparison to a negative control.

On the first instance observing Figure 24 we can extract the IC50 from the free diazoxide is 1350µM, extracted from the graph. Even though to have more precision on the IC50, there should be an approximation over the detected concentration, as for this experiment the tested concentration were set in a big range, so to follow up with this experiment a range of 2500µM and 500µM. As the cell viability over 2500 µM already reaches a low cell metabolic activity of 10,6% in comparison to the control group.

On the second experiment with MTT were the FND-HPG-DMA-Diazoxide concentrations are tested, the top two concentrations of ND (5 and 1 mg/ml), have been excluded from the analysis as the concentration was so high the confluence on the well on the 96 plate well plate, occluded the spectrophotometric analysis of those samples.

Over the second Figure 25 from the graph's equation the IC50 of the FND-HPG-DMA-Diazoxide is 0,175mg/ml FND equivalent, being proximate to the maximum concentration of FND-HPG-DMA-Diazoxide tested, in this case 0,2 mg/ml. observing this to get a more concrete analysis over the IC50, there should be an increase in volume and do the analysis over normal 35mm plates to have major resolution and obtain reassurance over the results.

DCFHDA

During the experimentation with the DCFHDA, the results where inconclusive, as the negative and positive controls didn't have the expected results. As on the first experiment described previously the negative control showcased higher activity of the ROS rather than the positive control with the hydrogen peroxide, the latter show a lesser signal than the samples itself. For which the signal on the positive control should be the highest obtained, and the negative the least, to be analyse the rest of the samples done and have set points to compare the ROS activation.

This contradicting result led to a second experiment done via the CLSM, as it will provide a higher resolution and precision than a fluorimeter. In this second experiment, a positive control with H_2O_2 was compared to a negative control with non-additives. All the same material was used as in the first experiment.

The results again where incoherent, as the negative control showed a higher signal on ROS than the positive control, that showed none. It is expected to observe ROS signal on the negative control, as cells by themselves will produce free radicals, but this signal shouldn't be higher than the positive control. Which led us to believe that the DCFHDA reactant was in bad state, thus should be changed.

Having a third experiment with the same methodology as before, but changing the medium and the DCFHDA reactant, in this case the medium of analysis will be 2%FBS with PBS, resulting in a clear solvent in which cell can survive still, and it won't interfere with the DCFHDA. As the DMEM is a read solvent may affect the reading of the signal in the fluorescence.

In the results obtained, we have an improvement as both negative and positive controls did provide a fluorescent signal. But the signal difference wasn't as different as expected.

This occurrence led to the conclusion that the H_2O_2 is not fit for a positive control in our case, in the use of the MDA-MB-231 cells, as this was test on other cell lines and it performed as expected. Then being possible that the hydrogen peroxide is in too low concentrations to induce a high ROS, or that is not compatible with our cells.

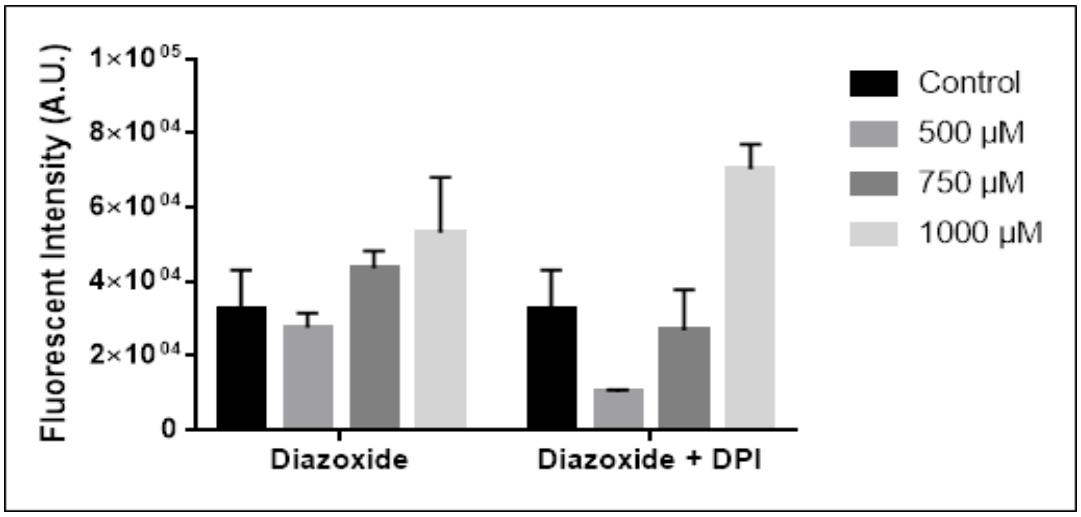

Figure 26: DCFHDA analysis, over three different concentrations of free diazoxide in the medium and free diazoxide with DPI, error bars show the standard deviation of the sample from 3 replicas.

In case we omit the results obtained on the first experiment from the ND (because of high concentration), and the positive control, because of invalid.

The results show (Figure 26) that the diazoxide can generate free radicals in the cells even when the ROS system is inhibited by the DPI, but as such the presence of ROS in the negative control is higher in both samples of 500 µM and 750µM, as in the negative control there was no inhibition from the DPI.

As we augment the diazoxide concentration on the cells the ROS signal is higher, therefore the oxidative stress induced. Although, observing the signal given by the sample which has 500 µM Diazoxide no PDI, the signal is lower than the negative control group, maybe requiring further experimentation around those diazoxide concentrations.

But as said the positive control was defective and the experiment should be repeated accordingly.

Conclusion:

- The creation of the polymer has been successful.
- HPG helps stabilize the ND surface charge making it more stable and aggregate less in physiological environment.
- The diazoxide can be used as anticancer drug for triple negative breast cancer therapy from MTT assay.
- Modification of diazoxide can increase the uptake of nanodiamond by cancer cells, where the endocytosis was blocked by HPG.
- And diazoxide can induce oxidative stress response, which provide the feasibility of using diamond magnetometry to detect this oxidative stress response precisely.
- The usage of the H_2O_2 as a positive control on the DCFHDA analysis needs further testing, as the results show that is not viable with the current treatment with MDA-MB-231

Going forward, to complete this pH-sensitive project, more experiments need to be added in the future:

(1) Different ratio of hydrophilic polymer with amino group (e.g. PEG) can be used to improve the size distribution of the nanomedicine.
(2) The pH sensitivity of DMA bond and drug release need to be added to support the project design.
(3) More cellular experiment including uptake of nanoparticles, and the final diamond magnetometry

In the end, we really hope our pH-sensitive drug delivery system based nanodiamond and diamond magnetometry can provide a new method to contribute to the drug screen via assessing cellular radical response.

Literature/References:

1. Nie L, Nusantara AC, Damle VG, et al. Quantum Sensing of Free Radicals in Primary Human Dendritic Cells. *Nano Lett*. 2022;22(4):1818-1825. doi:10.1021/acs.nanolett.1c03021

2. Nie L, Nusantara AC, Damle VG, et al. Quantum monitoring of cellular metabolic activities in single mitochondria. *Sci Adv*. 2021;7(21):1-8. doi:10.1126/sciadv.abf0573

3. Lobo V, Patil A, Phatak A, Chandra N. Free radicals, antioxidants and functional foods: Impact on human health. *Pharmacogn Rev*. 2010;4(8):118. doi:10.4103/0973-7847.70902

4. Abdal Dayem A, Choi HY, Kim JH, Cho SG. Role of oxidative stress in stem, cancer, and cancer stem cells. *Cancers (Basel)*. 2010;2(2):859-884. doi:10.3390/CANCERS2020859

5. Perevedentseva E, Hong SF, Huang KJ, et al. Nanodiamond internalization in cells and the cell uptake mechanism. *J Nanoparticle Res*. 2013;15(8). doi:10.1007/S11051-013-1834-8

6. Chu Z, Miu K, Lung P, et al. Rapid endosomal escape of prickly nanodiamonds: implications for gene delivery. *Sci Reports 2015 51*. 2015;5(1):1-8. doi:10.1038/srep11661

7. Schirhagl R, Chang K, Loretz M, Degen CL. Nitrogen-vacancy centers in diamond: Nanoscale sensors for physics and biology. *Annu Rev Phys Chem*. 2014;65:83-105. doi:10.1146/annurev-physchem-040513-103659

8. Zhao L, Takimoto T, Ito M, Kitagawa N, Kimura T, Komatsu N. Chromatographic separation of highly soluble diamond nanoparticles prepared by polyglycerol grafting. *Angew Chemie - Int Ed*. 2011;50(6):1388-1392. doi:10.1002/anie.201006310

9. Sun CY, Shen S, Xu CF, et al. Tumor Acidity-Sensitive Polymeric Vector for Active Targeted siRNA Delivery. *J Am Chem Soc*. 2015;137(48):15217-15224. doi:10.1021/jacs.5b09602

10. Maeda H, Nakamura H, Fang J. The EPR effect for macromolecular drug delivery to solid tumors: Improvement of tumor uptake, lowering of systemic toxicity, and distinct tumor imaging in vivo. *Adv Drug Deliv Rev*. 2013;65(1):71-79. doi:10.1016/J.ADDR.2012.10.002

11. Ko H, Son S, Jeon J, et al. Tumor microenvironment-specific nanoparticles activatable by stepwise transformation. *J Control Release*. 2016;234:68-78. doi:10.1016/j.jconrel.2016.05.009

12. Li XX, Chen J, Shen JM, et al. pH-Sensitive nanoparticles as smart carriers for selective intracellular drug delivery to tumor. *Int J Pharm*. 2018;545(1-2):274-285. doi:10.1016/j.ijpharm.2018.05.012

13. Huwaimel BI, Bhakta M, Kulkarni CA, Milliken AS. Discovery of Halogenated Benzothiadiazine Derivatives with Anticancer Activity **. 2021:1143-1162. doi:10.1002/cmdc.202000729

14. Virgili N, Mancera P, Wappenhans B, et al. K(ATP) channel opener diazoxide prevents neurodegeneration: a new mechanism of action via antioxidative pathway activation. *PLoS One*. 2013;8(9). doi:10.1371/JOURNAL.PONE.0075189

15. Ecacc M-. MCF-7 Cell line profile. *ECACC, Eur Collect Authenticated Cell Cult*. 2022;4(92020424):1-2. https://www.phe-culturecollections.org.uk/media/130237/mcf7-cell-line-profile.pdf.

16. Holliday DL, Speirs V. Choosing the right cell line for breast cancer research. *Breast Cancer Res*. 2011;13(4). doi:10.1186/BCR2889

17. Terada D, Sotoma S, Harada Y, Igarashi R, Shirakawa M. One-Pot Synthesis of Highly Dispersible Fluorescent Nanodiamonds for Bioconjugation. *Bioconjug Chem*. 2018;29(8):2786-2792. doi:10.1021/acs.bioconjchem.8b00412

18. Zhao C, Shao L, Lu J, Deng X, Wu Y. Tumor Acidity-Induced Sheddable Polyethylenimine-Poly(trimethylene carbonate)/DNA/Polyethylene Glycol-2,3-Dimethylmaleicanhydride Ternary Complex for Efficient and Safe Gene Delivery. *ACS Appl Mater Interfaces*. 2016;8(10):6400-6410. doi:10.1021/ACSAMI.6B00825/SUPPL_FILE/AM6B00825_SI_001.PDF

19. Gou J, Liang Y, Miao L, et al. Improved tumor tissue penetration and tumor cell uptake achieved by delayed charge reversal nanoparticles. *Acta Biomater*. 2017;62:157-166. doi:10.1016/J.ACTBIO.2017.08.025

20. Hopkins E, Sanvictores T, Sharma S. Physiology, Acid Base Balance. *Urolithiasis*. September 2021:19-22. doi:10.1007/978-1-4899-0873-5_4

21. Bouider N, Fhayli W, Ghandour Z, et al. Design and synthesis of new potassium channel activators derived from the ring opening of diazoxide: Study of their vasodilatory effect, stimulation of elastin synthesis and inhibitory effect on insulin release. *Bioorganic Med Chem*. 2015;23(8):1735-1746. doi:10.1016/j.bmc.2015.02.043

22. Kumar P, Nagarajan A, Uchil PD. Analysis of cell viability by the MTT assay. *Cold Spring Harb Protoc*. 2018;2018(6):469-471. doi:10.1101/pdb.prot095505

23. Invitrogen. Invitrogen-Molecular Probes Manual: Reactive Oxygen Species (ROS) Detection Reagents. *Mol Probes, Invit Detect Technol*. 2006:1-5. https://www.idexx.com/pdf/en_us/livestock-poultry/elisa-technical-guide.pdf.

24. Li Y, Trush MA. Diphenyleneiodonium, an NAD(P)H oxidase inhibitor, also potently inhibits mitochondrial reactive oxygen species production. *Biochem Biophys Res Commun*. 1998;253(2):295-299. doi:10.1006/bbrc.1998.9729

25. Lucitti JL, Sealock R, Buckley BK, et al. Variants of Rab GTPase-Effector Binding Protein-2 Cause Variation in the Collateral Circulation and Severity of Stroke. *Stroke*. 2016;47(12):3022-3031. doi:10.1161/STROKEAHA.116.014160

26. Goat anti-Rabbit IgG (H+L) Highly Cross-Adsorbed, Alexa Fluor™ Plus 405 (A48254). https://www.thermofisher.com/antibody/product/Goat-anti-Rabbit-IgG-H-L-Highly-Cross-Adsorbed-Secondary-Antibody-Polyclonal/A48254. Accessed July 5, 2022.

27. Fluorescence SpectraViewer. https://www.thermofisher.com/order/fluorescence-spectraviewer?SID=srch-svtool&UID=AF-Plus-405#!/. Accessed July 5, 2022.

28. Zs MZ, Nr S. Malvern ZetaSizer ZS Size ZS Size. 2008.

29. Zs MZ, Nr S, Srm N, et al. Malvern ZetaSizer ZS Zetapotential Malvern ZetaSizer ZS Zetapotential. 2008;(figure 1).

Acknowledgements:

First and foremost, I would like to thank my daily supervisor Kaiqi Wu, for the welcome into the project, the time and effort put forward to myself. It enabled me to be able to adapt quickly and understand the intricate parts of the project. I hope my work into the project will help him complete his PhD thesis, at which I whish him the best of luck.

I would like to thank as well Dr.prof. Romana Schirhal, and the Bioimaging & Bioanalysis team, I felt welcome since the first day, and my opinion and input has always been valued, making me one more of the team, making the experience far more valuable and for which I'm grateful.